land

MDPI

Article

Research on the Influence Mechanism of Street Vitality in Mountainous Cities Based on a Bayesian Network: A Case Study of the Main Urban Area of Chongqing

Hongyu Wang [1], Jian Tang [2], Pengpeng Xu [1,*], Rundong Chen [1] and Haona Yao [1]

[1] School of Management Science and Real Estate, Chongqing University, Chongqing 400044, China; 202016131312@cqu.edu.cn (H.W.); 201703021070@cqu.edu.cn (R.C.); haonayao@cqu.edu.cn (H.Y.)
[2] Chongqing Design Institute, Chongqing 400044, China; cqadi@cqadi.com.cn
* Correspondence: xupp@cqu.edu.cn

Abstract: As the main spatial carrier for people's social activities, street space occupies an important position in the urban space. However, under the direction of traffic-driven urban planning, the social function of street space has been neglected, resulting in the gradual loss of vitality. In mountainous cities with rugged terrain, the factors influencing the vitality of streets may be different compared to those in plain areas. In order to explore the influence mechanism of street vitality in mountainous cities, a new quantitative research method based on the new data environment and a Bayesian network is proposed. In this study, Python and GIS are used to obtain spatial data of streets, and Bayesian networks are used to construct street vitality models to identify important influencing factors and causal relationships between influencing factors. The results demonstrate strong causal dependencies between the factors influencing street vitality in mountainous cities. The mechanism of influence of street vitality revolves around functionality and street texture in terms of its own environment and external environment, respectively. The combination of factor group with functional density as the root node achieved the maximum probability of high vitality of the street. The results of this study have implications for community or urban planners with respect to urban regeneration and street vitality promotion.

Keywords: street vitality; influence mechanism; Bayesian network; multisource data; urban regeneration

Citation: Wang, H.; Tang, J.; Xu, P.; Chen, R.; Yao, H. Research on the Influence Mechanism of Street Vitality in Mountainous Cities Based on a Bayesian Network: A Case Study of the Main Urban Area of Chongqing. *Land* **2022**, *11*, 728. https://doi.org/10.3390/land11050728

Academic Editor: Fabrizio Battisti

Received: 28 March 2022
Accepted: 7 May 2022
Published: 12 May 2022

1. Introduction

In the early 1930s, modern urban planning represented by the *Athens Charter* advocated functional zoning cities and attached importance to the organization and efficiency of transport. However, the excessive pursuit of large-scale and monolithic functional zoning had rendered cities rigid and monotonous. Buildings had become isolated units, and the original diversity of urban life had become monotonous. After the gaps in theory of modern urban planning were exposed, Jacobs (1961) pioneered the concept of "street vitality", emphasizing the important role of the street in the city [1]. She believed that "when streets are vibrant, cities are vibrant, and when streets are boring, cities are boring". That means mixed usage of streets, small street sections, buildings of different eras and dense pedestrian traffic can create vibrant streets. "Vitality" is a kind of non-physical spatial quality that is hardly measurable. Lynch (1979) argued that urban vitality includes continuity, security, harmony and stability throughout the whole ecosystem.

Previous research on urban spatial vitality has mainly focused on the formation of vitality from two aspects. On the one hand, there exist some simple measurable or evaluable external representations, namely human activities [2,3]. Previous studies primarily used traditional techniques such as questionnaires, interviews, field surveys and photographic records to collect data [4–6]. As this type of method requires a considerable investment of time, manpower and financial resources, data acquisition is difficult. Therefore, most

studies using this type of data acquisition method only focus on one or several typical streets, making it difficult to expand the research scope. With the development of big data technology, mobile phone data [7,8], social media sign-in data [9–11] and other local-based service (LBS) data have gradually been applied to research of urban spaces. Such big data have significant advantages, such as extensive spatial coverage and rich human information. Traditional methods, such as field surveys and questionnaires, have been gradually replaced. As an Internet external location-related technology, LBS data perform clustering calculations according to location, and the degree of clustering presented can reflect the degree of street vitality to a certain extent [12], which has been widely used by the academic community because of its high resolution and relatively open API. Scholars have used LBS data for studies in domains such as urban vitality [13].

On the other hand, research on street vitality concerns the street space that sustains human activities, and scholars have focused more on the factors of street vitality [3]. Research on the factors that influence street vitality have primarily been conducted from the perspective of the two aspects of macroenvironment and microenvironment. The dimension of the macroenvironment mainly included location [14], accessibility [8,15], surrounding land development intensity [16–19] and street texture [20–22]. Even within the same neighborhood, however, there are substantial variances in street usage, with some streets being more vibrant than others. Analysis of street vitality from a macrodimensional perspective is obviously insufficient because it ignores the impact of micromaterial environmental characteristics. At the micro level of the street, the main factors influencing the vitality of the street include comfortability [23–25], mixed use of functions [3,26] and safety [6]. In the era of big data, POI data [17,27], street view data [28–30] and other new types of multisource data are being introduced into the study of urban vitality to carry out more detailed cross validation.

It is worth noting that the dimensions of city types were distorted in earlier research on street vibrancy. Existing studies, on the other hand, revealed that different types of cities performed differently under the same urban vitality evaluation index system [8,31]. Furthermore, there is a dearth of in-depth data analysis of the causal relationship between the elements impacting street vitality in the available studies.

In addition, mountain city road networks and plain road networks are very different. First, plain city road network distribution is more orderly, mostly in grid layout. Second, the travel distance within mountain city groups is short, whereas the travel distance between groups is long. Third, mountain city street slope is large, the relative height difference is large, and in order to adapt to the terrain, the road network is more broken. As a typical mountain city, Chongqing was chosen as the research object in this study.

This study proposed a framework to describe the causal relationship and influence mechanism of the factors of street vitality in mountainous cities. Following questions were answered: (1) What are the important factors influencing the vitality of mountainous city streets? (2) What causal relationship does the influencing factors of street vitality follow in mountainous cities? (3) How do the influencing factors affect street vitality in mountainous cities?

The rest of the paper is structured as follows. Section 2 presents the methodology of the study in detail. Section 3 presents the selection of Bayesian network nodes and the data used for the study. The analysis results are presented in Section 4. Section 5 provides a discussion and conclusions.

2. Methodology

This study is divided into three steps: First of all, the factors influencing street vitality in mountainous cities were screened with reference to existing studies. Subsequently, multisource city big data were used to quantify the indicators of street vitality factors, including LBS data, POI data, street view image data, building outline data and road network data. Furthermore, Bayesian networks were introduced to construct a model of street vitality impact in mountainous cities using structural learning and parametric

learning methods. Finally, in order to explore the mechanism of street vitality influence in mountainous cities, the causal relationships among street vitality influencing factors and the optimal factor combination groups were identified through structural analysis, single-factor analysis and multifactor combination analysis.

Bayesian networks can be used to define causal effects of external interventions and describe causal relationships between multiple variables. To date, Bayesian networks have been used in many fields to solve practical problems, such as industrial control [32], medical diagnosis [33,34], environmental management [35,36], etc.

According to a review of previous studies, the methods of causal inference include regression models, path analysis, structural equation models, dual difference, breakpoint regression, tendency value matching, instrumental variable methods, etc. Based on big data, this study wants to determine the causal relationship between the influencing factors of street vitality from an objective perspective with a data-driven approach rather than verifying the causal relationships based on a subjective experiential hypothesis. Therefore, regression models, path analysis methods and structural equation models are not applicable to this study. In the study of street vitality, to carry out large-scale measurement, it is difficult to find a sufficient number of experimental and control streets that meet the requirements, and the data used in this paper are not panel data, so dual difference, breakpoint regression, propensity value matching and instrumental variable methods are not applicable.

Therefore, in this study, we combined Bayesian networks with GIS data. Research on combining Bayesian networks with GIS data is also emerging [37,38]. The Bayesian network–GIS framework has been demonstrated to be a practical tool [39]. In this study, basic concepts of Bayesian networks, BN node selection and data collection will be introduced.

2.1. Bayesian Network

A Bayesian network (BN), also known as a belief network, is the product of the combination of Bayesian theory and graph theory. Such networks are often used to solve uncertain problems in complex systems and to mine causal relationships from data. Given a finite set of variables, V = [25 . . . Vn], X denotes a directed arc between different variables in the set, V. After passing through a number of directed arcs from any node, none of them can return to the original node. Then, G = <V, X> is called a directed acyclic graph. Directed acyclic graphs intuitively show the complex relationships between nodes in a qualitative way. The quantitative part of a Bayesian network is represented by a table of conditional probabilities (CPT) representing each node, Vi, under the conditions of its parent set of nodes, called a Bayesian parameter Θ. A Bayesian network can be represented as N = <G, Θ>. A variety of algorithms support the construction of Bayesian networks from data learning. There is a range of terminology used to describe the Bayesian network modelling process and the analysis of results [40]. A list of terminology related to Bayesian networks used in this paper is given in Table 1.

Table 1. Explanation of terms related to Bayesian networks.

Terminology	Meaning and Examples
Node	Refers to variables in the BN model. They can be either discrete or continuous.
Arc	The directed arrow between nodes indicates direct influence between two nodes.
State	Refers to the different values of the node variables.
CPT	Demonstrates the conditional probability of each node under the influence of its parent node set, reflecting the strength of the causal relationship.
Parent Node	In simple terms, represents the cause node. If there is a directed arc between two nodes, then the one emitting the arrow is said to be the parent node.
Child Node	In simple terms, represents the result node. If there is a directed arc between two nodes, then the one pointed to by the arrow is said to be a child node.
Descendant Node	Any node that a node can reach through a directed chain is called the descendant node of that node.

Table 1. *Cont.*

Terminology	Meaning and Examples
Root Node	When a node has only descendant nodes and no parent node, the node is said to be the root node in the BN.
Ancestor Node	Any node that points to a node through a directed chain is called an ancestor nodes of that node.
Evidence Node	When the actual state of a node is observed or some decision is made for that node, setting that node as an evidence node, it can only have a unique value with probability 1 at that point.
Target Node	When performing inference, only certain nodes in the network may be of interest. By setting these nodes as targets, only updates to the target nodes are observed when inference is performed, given the evidence nodes. When no target node is set, all nodes are targets by default.

2.2. Modeling and Validation of Bayesian Network Model for Street Vitality in a Mountain City

When performing BN learning, severe multicollinearity between variables is not allowed; otherwise, incorrect analytical results maybe caused [41]. Therefore, the multicollinearity test needed to be performed before modeling. Variance inflation factor (VIF) is the most commonly used inspection variable. It is generally believed that when VIF > 10, there is a serious multicollinearity problem [42]. After eliminating the multicollinearity problem, the influencing factors need to be discretized.

Most Bayesian networks are modeled for discrete variables, and the model construction and operation of discrete random variables are faster and more accurate. Therefore, after the node variables are determined, the variables are discretized. The number of states of a variable is usually a compromise between model precision and simple degrees. In order to improve the overall accuracy of the network and reduce the cost of calculation, continuous variables are discretized into three states at most [43].

During modeling, streets covered by Baidu Street View were selected as samples to ensure the integrity of data of each variable. A total of 3284 data samples were used to construct the Bayesian network. According to the data characteristics of the variables selected in this paper, the average thermal value was divided into two parts by quantile classification method, and 1 (low) and 2 (high) were assigned. The data of each explanatory variable were divided into 3 groups by natural discontinuity grading method, and values 1, 2 or 3 were assigned to each group according to numerical size from small to large. The discretization method is shown in Appendix A.

Next, the BN model was formally built with the help of Genie software, which mainly included BN structure learning, BN parameter learning and model verification. The purpose of BN structure learning is to determine the optimal network topology that can reflect the relationship between variables to form a directed acyclic graph between nodes, which is the qualitative part of Bayesian network learning. In this study, a PC algorithm based on conditional independent test method [44] was used to calculate and learn structures of the Bayesian network, integrating expert knowledge for a few adjustments. BN parameter learning is based on the network structure to learn the conditional probability distribution of each node through a given data set. An EM algorithm [45,46] that can perform calculations under the condition of missing values was used for parameter learning in this study.

In order to ensure its correctness and validity, the constructed model needed to be verified. In this paper, the K-fold cross test [47] was used to verify the model, and the performance of the model was evaluated by two parameters. The first parameter is the F-score [48]. The second parameter is the area under the ROC (receiver operating characteristic) [49], also known as the sensitivity curve. The horizontal axis is the false-positive rate, and the vertical axis is the true positive rate. The Area under the ROC curve (AUC) is generally not less than 0.5. When $0.5 \leq AUC < 0.6$, the model performance is poor. When $0.6 \leq AUC < 0.7$, the model performance is medium. When $0.7 \leq AUC < 0.8$, the model performance is good. When $0.8 \leq AUC < 0.9$, the model performance is great. When $AUC \geq 0.9$, the model performance is excellent.

3. BN Node Selection and Data Collection

3.1. BN Node Selection

For Bayesian network modeling, the external indicators of street vitality and some important factors influencing street vitality were defined as node variables. Street vitality is embodied by human activity density. Based on previous studies [12,13], the population activity density reflected by Baidu's LBS data was used as a measure of the external manifestation of street vitality, expressed by MHV.

Many studies have measured the impact of factors on the vitality of streets. From the perspective of social interaction, Gehl (2010) analyzed the activities of people on streets and concluded that the spatial elements of good streets are: "small-scale street detail planning and richness design of building facades", which is in line with W. Wu et al. (2016), who stated that, "increasing road density will encourage human travel and regular activity, thus fostering future vitality". The research of Lin and Moudon (2010) showed that the closer the streets of the city center, the regional center or large-scale commercial complex compound, the stronger the radiation effect is, and the vitality of the street is also relatively higher. Ewing et al. (2016) conducted a large number of evaluation studies on the construction of urban spaces and walkability, and their results suggest that accessibility is one of the key guarantees of vibrant streets, which coincides with the conclusion of Tu et al. (2020). Mehta (2007) and Xu et al. (2018) conducted quantitative research on road connectivity and street vitality. Montgomery (1998) proposed that land functions, shops, scale and type of business, price and quality, squares and open spaces, mixed use of land, diversity of commercial configuration, architecture and street life are the key elements that determine the vitality streets. In terms of land development intensity and the impact of mixed land use on urban vitality, both studies that suggest it has a positive effect [18,19] and studies that suggest it has a negative effect [16,50] have been reported. In terms of the environmental comfort of streets, studies by Borst et al. (2008) and Sarkar et al. (2015) indicated a positive association between walking attractiveness and street tree cover or green view rates. Openness refers to the proportion of the sky area that is visible from a particular viewpoint to the entire field of view, which affects the length and degree of sunlight exposure of a street, thus influencing the microclimate environment of streets and people's perception of vision [51]. A boundary and enclosed space can provide users with a more intimate and private place, making them feel protected, providing them with a sense of security and meeting their safety needs [52]. Research by Ewing et al. (2005) also showed that the degree of enclosure is related to street vitality.

For targeted research on mountain cities, it is necessary to fully consider their characteristics, such as low density, discontinuity, low accessibility, infringement of ecological space, special spatial structure, etc. Urban elevation information was supplemented, and the average elevation and longitudinal slope of streets were calculated in this study, which can help to reflect the characteristics of urban streets in mountainous areas. It was not difficult to understand that slope affects how people feel about using streets. On the one hand, slopes that exceed certain limits cause inconvenience to people, especially the elderly, the disabled and women with small children. On the other hand, street features such as slopes and stairs were positively associated with perceived attractiveness [23].

Based on existing studies, the influencing factors of street vitality in mountainous cities screened in this study are shown in Table 2, which include the eight aspects of horizontal interface characteristics, comfortability, mixed use of function, safety, location, accessibility, intensity of surrounding development and street texture, with a total of 18 factors.

Table 2. Influencing factors and quantitative methods of street vitality in mountainous cities.

Perspective	Influencing Aspects	Influencing Factors	Symbol	Quantification Methods	Discretization Classification
Street characteristics	Horizontal interface characteristics	Street length	SLen	Calculated by Arcgis	short, moderate, long
		Elevation *	MEle	Calculated by Arcgis	low, moderate, high
		Longitudinal slope *	SLO	Average height difference/street length	low, moderate, high
	Comfortability	Green view ratio	GVR	Area of greenery/area of streetscape	low, moderate, high
		Sky view ratio	SVR	Area of sky/area of streetscape	low, moderate, high
	Mixed use of function	Functional density	FDen	Number of POIs/street length	low, moderate, high
		Functional diversity	FDiv	Shannon entropy of the POI category	low, moderate, high
	Safety	Surround close ratio	SCR	Vertical enclosure area/street view area	low, moderate, high
		Lighting facilities	LFac	/	none, exist
	Location	Distance to the nearest commercial center	BcDis	Calculated by Arcgis	near, moderate, far
		Distance to the nearest shopping mall	SmDis	Calculated by Arcgis	near, moderate, far
Surrounding environment	Accessibility	Density of bus stops	BsDen	Number of stops/length of streets	low, moderate, high
		Density of bus lines	BrDen	Line length/street length	low, moderate, high
		Distance to the nearest metro station	MsDis	Calculated by Arcgis	near, moderate, far
		Road density	RDen	Total length of roads in the buffer zone/ 1 km buffer zone area	low, moderate, high
	Intensity of surrounding development	Building density	BDen	Building footprint/50 m buffer area	low, moderate, high
		Building floor area ratio	FAR	Building floor area/50 m buffer zone area	low, moderate, high
	Street texture	Intersection density	IDen	Number of intersections/ 1 km buffer zone area	low, moderate, high

Note: "*" refers to influencing factors with characteristics of mountain cities.

3.2. Data Collection

Chongqing city is a typical mountain city. The area west of Nanshan within the inner ring of the main urban area of Chongqing was selected as the research area, with a total area of about 233 km^2, as shown in Figure 1. The road network in the research area is complex and interlaced, with the following three characteristics: (a) The trip distance within the city cluster is short, and the trip distance between clusters is long. (b) The street has a large slope and a large relative height difference. (c) In order to adapt to the terrain, the road network has many interruptions. Chongqing was selected as a representative case to study the vitality of mountainous city streets.

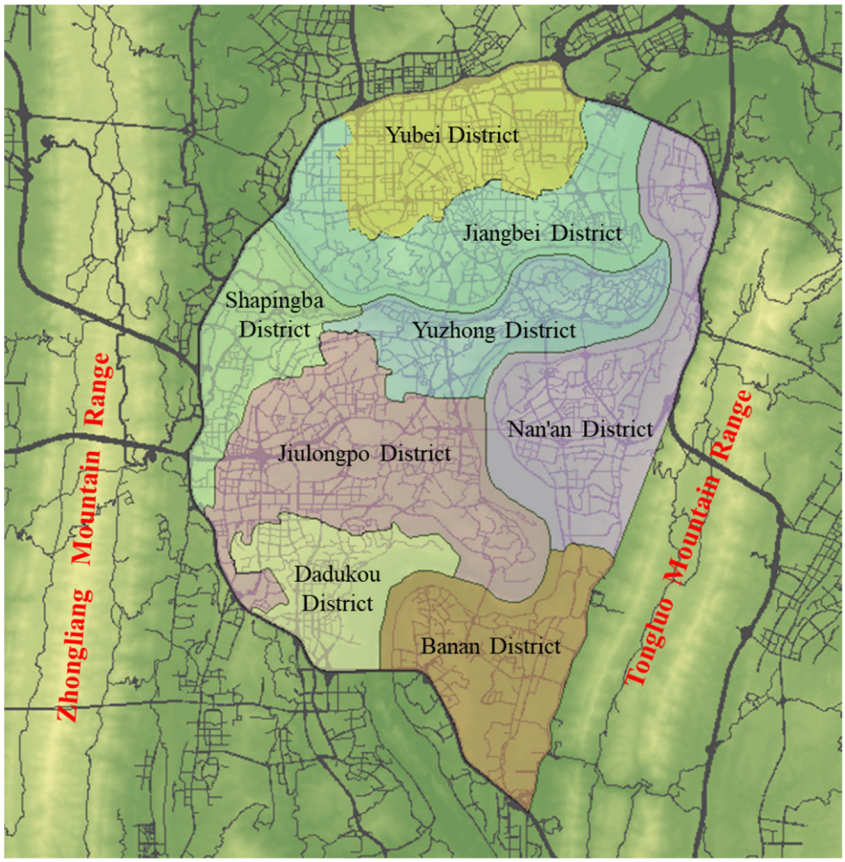

Figure 1. Research scope.

The data required for this study include road network data, building data, elevation data, bus route data, POI data, street view image data and LBS data, as shown in Table 3. (1) The road network data are the basic data of this study. After processing, the simplified road network (Figure 2, left) and the buffer zone generated 50 m along the center line of the road (Figure 2, right) were obtained. In order to facilitate data analysis, the street segments between intersections were taken as the smallest research unit in this study. With a total of 3621 street segments, each street segment was assigned a unique ID. (2) The urban building vector data included the three basic data points of building outline, building base area and building height. A total of about 302,700 building data points were obtained within the research scope. (3) Elevation data were in the form of raster data, and elevation points were generated in Arcgis at 5 m intervals. Then, the elevation points within the 10-m buffer zone to the left and right of the road centerline were connected with the street buffer zone to obtain the elevation point data of each street segment, totaling about 865,300 elevation points. (4) The bus route data comprised Chongqing's bus routes in 2019. After cropping in ArcGIS, a total of 380 bus routes were obtained in the buffer zone of the study area, with a total length of about 4877.62 km. (5) POI data of 16 major categories related to residents' daily life and work were obtained, with a total of 183,489 POI points, as shown in Figure 3. (6) Streetscape images obtained with on Python were visually screened, and after removing images that did not meet our requirements, such as bridges and culverts, 36,387 images were ultimately used for image semantic segmentation. There were 19 categories of labels for semantic segmentation of streetscape images, as shown in Figure 4. (7) Four days (two weekdays and two rest days) with good weather and suitable temperature were selected to collect Baidu LBS data from 7:00 am to 24:00 pm with 30 min intervals. A total of 136 data maps were collected, and the data were processed in Arcgis, as shown in Figure 5.

Table 3. Required data for street vitality research.

Vitality Measurement Indicators/Influencing Factors	Data Support	Data Sources
MHV	LBS data	Baidu map
SLen RDen IDen	Road network data	Open street map
MEle SLO	Elevation data	Geospatial data cloud
GVR SVR SCR LFac	Street View image data	Baidu map
FDen FDiv BcDis SmDis MsDis BsDen	POI data	Baidu map
BrDen	Bus route data	City data group
BDen FAR	Building vector data	A map

Figure 2. Road network and buffer zone after processing.

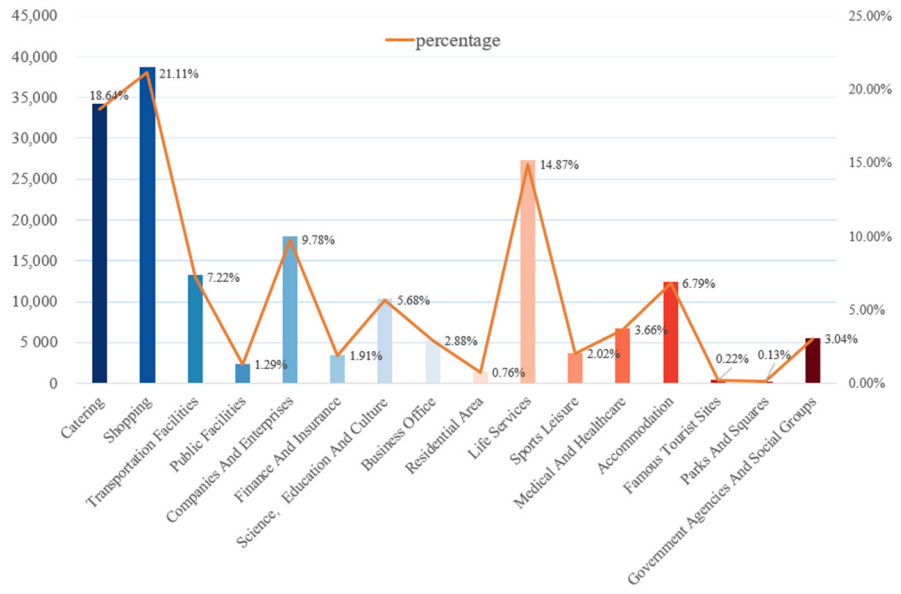

Figure 3. Statistics of the number of classified POIs.

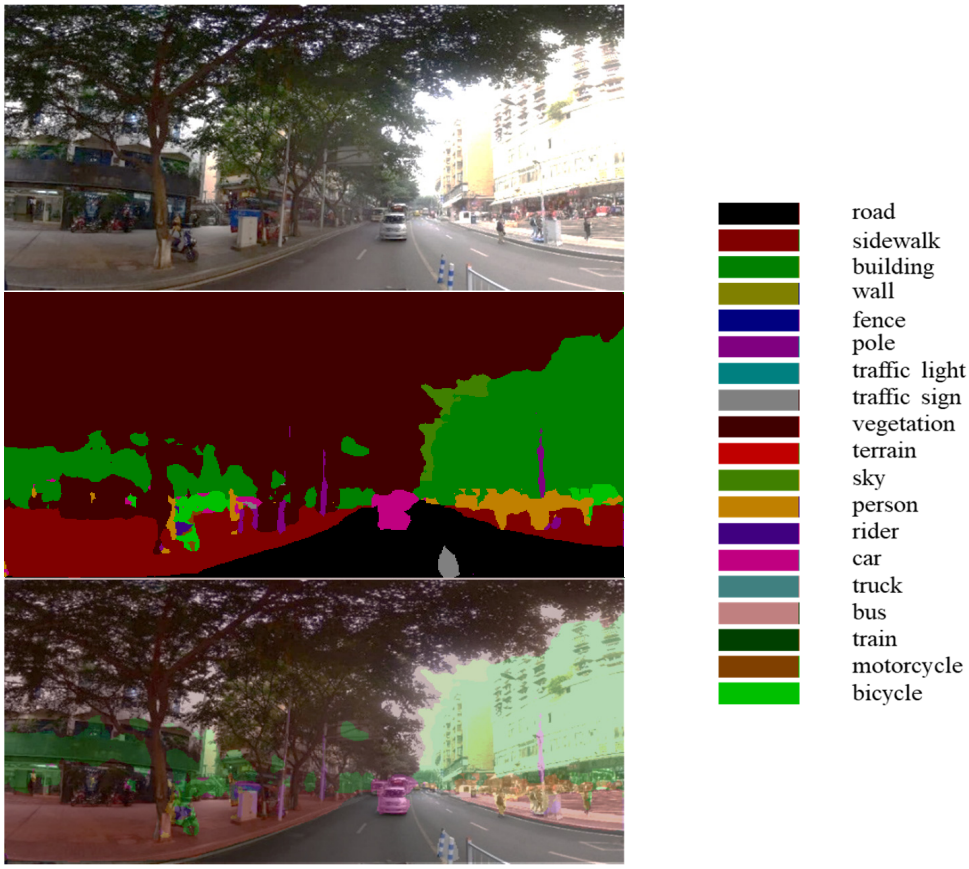

Figure 4. Results of image semantic segmentation.

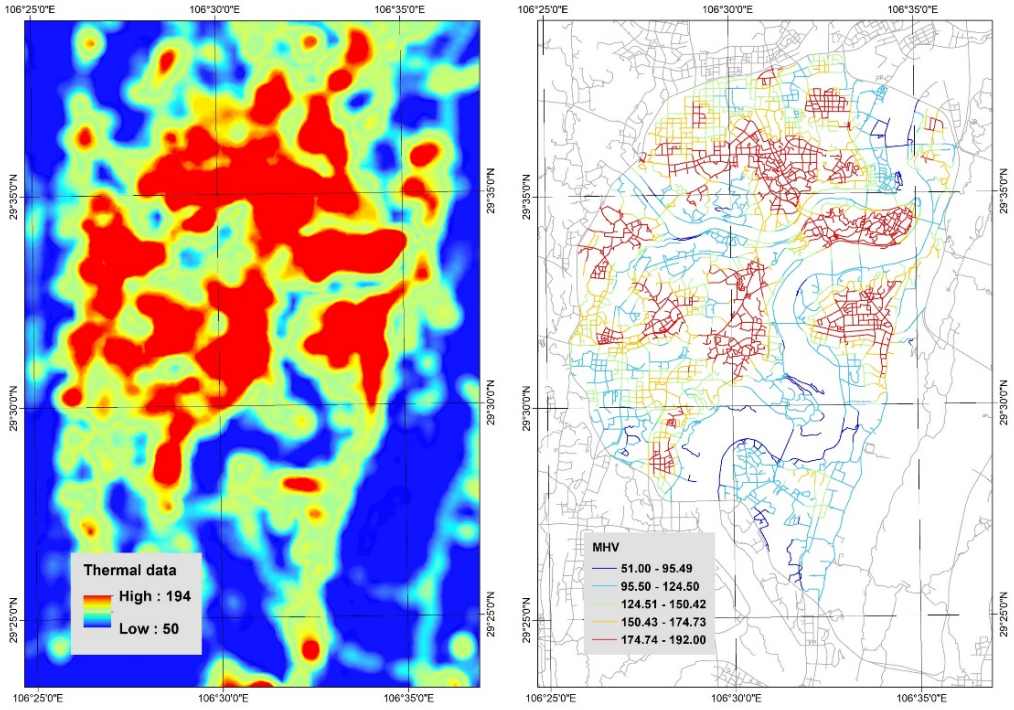

Figure 5. Comparison of heat map data before and after processing (**left**: heat map data before processing; **right**: heat map data after processing).

From the point of view of space, street vitality shows obvious polycentric distribution characteristics, radiating outward from the city center and the city subcenter. Yuzhong Peninsula and the surrounding area, with Guanyinqiao as the core, showed a high vitality level, followed by Nanping, Yangjiaping-Daping, Three Gorges Square and the surrounding area of Chaoyang Park. In other areas, the street vitality and the central area present a large gap. According to our analysis, every district except Banan district has at least one vitality pole.

4. Results

Two tests of multicollinearity were conducted in this study, and the results are shown in Table 4. The results of the first calculation show that the VIF1 of both SVR and SCR were greater than 10, proving the existence of severe multicollinearity. Therefore, after excluding the SVR with the largest VIF1, the multicollinearity needed to be calculated again for the remaining 17 influencing factors. The second calculation results show that after SVR was removed, the VIF2 of all factors was less than 10, proving that there was no serious multicollinearity. Therefore, the above 17 factors can be used as network node variables for the BN structure, and MHV was also included in the network. In this study, GeNIe was used to conduct Bayesian network modeling. We imported the processed data set into GeNIe and used a PC algorithm to learn the structure and set parameters. Because the node variables used in this paper are discrete, representing, at most, three states, a discrete threshold of 3 was selected, i.e., variables with more than three parameters of different values were considered continuous. After the network structure was determined, the EM algorithm was used for Bayesian network parameter learning with the given sample data, and the conditional probability table was obtained. K-fold cross validation was performed on the BN model obtained through structure and parameter learning. The results of F1 score and AUC are shown in Table 5, indicating good performance of the BN model constructed in this study.

Table 4. Results of two multicollinearity tests.

Variables	SLen	Mele	SLO	GVR	SVR	FDen	FDiv	SCR	LFac	BcDis	SmDis	BsDen	BrDen	MsDis	RDen	BDen	FAR	IDen	Mean VIF
VIF1	1.41	1.29	1.16	2.78	14.83	1.64	1.65	14.5	1.02	2.17	1.68	1.09	1.23	1.19	6.09	2.41	2.46	6.83	3.64
VIF2	1.4	1.28	1.16	2.75	/	1.6	1.61	3.61	1.02	2.13	1.68	1.09	1.23	1.19	6.08	2.4	2.46	6.83	2.33

Table 5. BN model verification results.

	F1-Score	AUC
MHV = High	0.9195	0.9693
MHV = Low	0.9191	0.9693

4.1. BN Structure Analysis

The Bayesian network structure is shown in Figure 6. MEle, SLO and Fden were the root nodes in the structural network without parent nodes. MHV had direct dependencies with all the remaining 11 node variables, except SLO and SCR. The dependencies between all node variables were interleaved, resulting in a slightly complex network.

The factor cluster with MEle as the root node (Figure 7a) contained 10 nodes: MEle, SCR, BrDen, MsDis, RDen, SmDis, BcDis, BDen, IDen and MHV. These ten nodes were interleaved with many directed arcs and formed a total of 23 paths. The factor cluster with SLO as the root node (Figure 7b) contained seven nodes: SLO, IDen, RDen, SmDis, BcDis, MsDis and MHV. These seven nodes formed a total of eight paths. The factor cluster with FDen as the root node (Figure 7c) contained 11 nodes: FDen, FDiv, BDen, FAR, SCR, IDen, RDen, MsDis, SmDis, BcDis and MHV. The dependency relationships among these 11 nodes were relatively interleaved, forming a total of 16 paths.

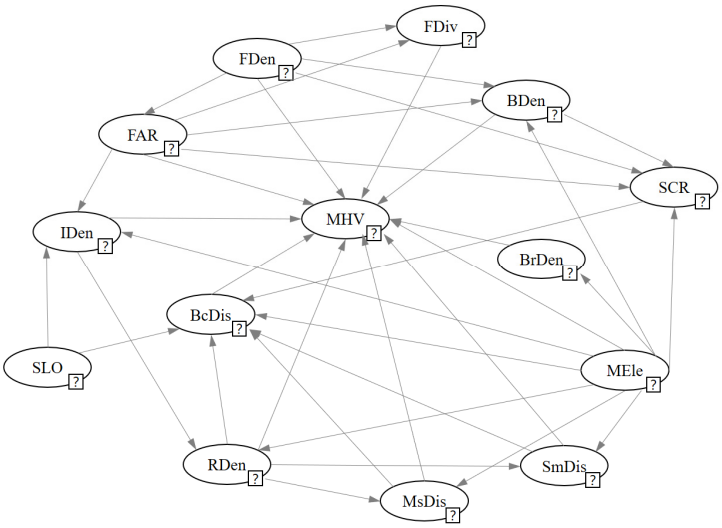

Figure 6. Final Bayesian network structure (note: the three factors of BsDen, GVR and LFac are not related to any other factors in the results, so they are not displayed in the network structure).

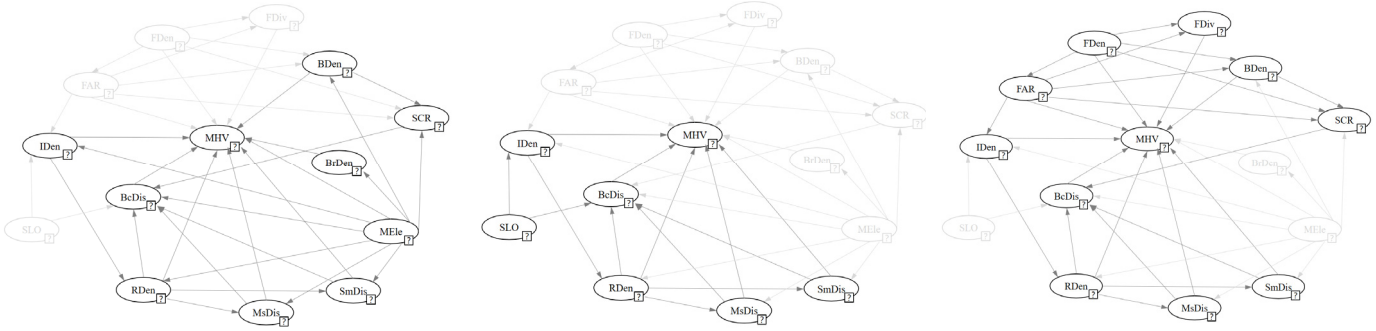

(**a**) (**b**) (**c**)

Figure 7. Factor group structure of different root nodes. (**a**) MEle as the root node; (**b**) SLO as the root node; (**c**) FDen as the root node.

4.2. Single-Factor Analysis

4.2.1. Forward Inference

In order to quantify the degree of influence of each influencing factor on street vitality, the BN model was used to carry out forward inference. Forward inference refers to a posteriori probabilistic inference from cause to effect. The influencing factor node was set as an evidence variable (denoted as E) and assigned a state. Through probabilistic inference, the posterior probability distribution of the query variable (denoted as Q) under a certain state of the influencing factor was obtained. In this section, an associative tree algorithm [53] was used to carry out forward inference with MHV as the query variable.

The single-factor forward inference results are shown in Table 6. The posterior probabilities of query variables in different states of each evidence variable were compared to determine the degree of influence of evidence variables on street vitality. The results show that factors with the large influence were IDen and RDen, followed by FDiv, MEle, SmDis and FAR; those with intermediate influence were BcDis, BDen, FDen, SCR and MsDis; and those with relatively small influence were SLO and BrDen.

Table 6. Extent of influence of evidence variables on street dynamics.

E	Q	Initial Probability of Q	Posterior Probability of Q			Probability Increase Value
			E = 3	E = 2	E = 1	
MEle	MHV = High	0.4909	0.4736	0.5350	0.4193	0.1157
SLO			0.5406	0.5035	0.4844	0.0562
FDen			0.4664	0.4466	0.5421	0.0955
FDiv			0.4789	0.5179	0.5945	0.1156
SCR			0.4663	0.5034	0.5615	0.0952
BcDis			0.5475	0.5490	0.4491	0.0984
SmDis			0.5748	0.5442	0.4645	0.1103
BrDen			0.4762	0.4926	0.5183	0.0421
MsDis			0.5655	0.5160	0.4827	0.0828
RDen			0.4323	0.4777	0.5783	0.1460
BDen			0.4242	0.4492	0.5456	0.0963
FAR			0.4146	0.4157	0.5295	0.1138
IDen			0.3983	0.4809	0.5744	0.1761

Note: the three states of the evidence variable (E): 1 = Low/Near, 2 = moderate, and 3 = High/Far. The probability increase represents the difference between the maximum and minimum probabilities in posterior probability.

4.2.2. Sensitivity Analysis

GeNIe provides a sensitivity analysis function, with the depth of red reflecting the strength of sensitivity. The sensitivity coefficient is displayed next to the node. The larger the coefficient, the higher the sensitivity. The MHV node was set as the target node for sensitivity analysis. The results are shown in Table 7. The sensitivity of street vitality to each node variable was divided into six echelons from high to low. (1) The first echelon included FDen, MEle and FAR, with the strongest sensitivity. (2) The second echelon included SLO. (3) The third echelon included SmDis, FDiv, FDen and IDen. (4) The fourth echelon included BDen, BrDen and MsDis. (5) The fifth echelon included BcDis. (6) The sixth echelon included SCR. Combined with the analysis of the Bayesian network structure, it can be seen that the descendants a node has, the higher the sensitivity. For example, MEle was the root node in the network structure. In addition to street vitality, MEle still had eight descendant nodes, seven of which were directly dependent on street vitality. Furthermore, there were 22 paths between MEle and MHV. Changes in MEle caused changes in many other factors, which were gradually transmitted through the paths. All the subtle changes converged together have a greater impact on the vitality of the street. FDen and FAR also had many descendant nodes, and there were many paths between them and MVH. On the contrary, both BcDis and SCR had only one descendant node of MHV, and their changes had no impact on other nodes and did not produce compound effects, so their sensitivity was weak.

Table 7. Sensitivity ranking.

Nodes	Sensitivity Coefficient	Ranking
FDen	0.0934	1
MEle	0.0908	2
FAR	0.0743	3
SLO	0.0508	4
SmDis	0.0262	5
FDiv	0.0227	6
RDen	0.0197	7
IDen	0.0191	8
BDen	0.0175	9
BrDen	0.0173	10
MsDis	0.0147	11
BcDis	0.0061	12
SCR	0.0028	13

4.3. Multifactor Combination Analysis

Street vitality is usually caused not by a single factor but by a combination of multiple factors. Based on the analysis of the influence of individual factors, we studied the probability distribution of street vitality under the combination of multiple factors. Based on the BN structure, all the paths leading to the MHV node were determined, starting from the root node. Because of the interactions of the nodes along a path, multiple factors on the path were called to the factor combination group. The annealing MAP algorithm was used to calculate the influence of different factor combinations on the posterior probability of street vitality.

The results of the multifactor combination analysis are shown in Table 8. Figure 8 shows the longest path from each root node; generally the more nodes included, the greater the posterior probability of high vitality of the street. Among the 46 factor combinations, the most likely combination to create a high-vitality street was composed of six factors: FDen, FAR, IDen, RDen, SmDis and BcDis (Figure 8c), covering mixed use of function, development intensity, location and street texture. It should be noted that this is only the longest path in the group of factors. In fact, the influence of each node on MHV was not only transmitted through this path; there were cross effects between each node, such as the influence of RDen on SmDis and the direct effect of each node on MHV. Among the factor combination groups from different root nodes, the factor combination group with FDen as the root node had the best overall performance in terms of high street vitality, followed by the factor combination group with MEle as the root node, although the difference between them was not significant. The factor combination group with SLO as the root node performed poorly.

Table 8. Analysis of factor combination groups.

Root Node	Number	Evidence (E)	MAP	P (MAP | E)	Degree of Influence	Group Ranking	Overall Ranking
MEle	1	MEle = M, IDen = H, RDen = H, MsDis = N, BcDis = N	MHV = H	0.7763	0.2854	1	3
	2	MEle = M, IDen = H, RDen = H, SmDis = N, BcDis = N	MHV = H	0.7734	0.2825	2	5
	3	MEle = M, IDen = H, RDen = H, BcDis = N	MHV = H	0.7509	0.2600	3	6
	4	MEle = M, IDen = H, BcDis = N	MHV = H	0.7365	0.2456	4	7
	5	MEle = M, RDen = H, SmDis = N, BcDis = N	MHV = H	0.7018	0.2109	5	11
MEle	6	MEle = M, RDen = H, MsDis = N, BcDis = N	MHV = H	0.6943	0.2034	6	12
	7	MEle = M, RDen = H, BcDis = N	MHV = H	0.6873	0.1964	7	14
	8	MEle = M, IDen = H, RDen = H, SmDis = N	MHV = H	0.6669	0.1760	8	18
	9	MEle = M, BDen = H, SCR = H, BcDis = N	MHV = H	0.6668	0.1759	9	19
	10	MEle = M, IDen = H, RDen = H, MsDis = N	MHV = H	0.6595	0.1686	10	21
	11	MEle = M, IDen = H, RDen = H	MHV = H	0.6433	0.1524	11	25
	12	MEle = M, SmDis = N, BcDis = N	MHV = H	0.6376	0.1467	12	27
	13	MEle = M, IDen = H	MHV = H	0.6319	0.1410	13	29
	14	MEle = M, MsDis = N, BcDis = N	MHV = H	0.6055	0.1146	14	31
	15	MEle = M, RDen = H, SmDis = N	MHV = H	0.6048	0.1139	15	32
	16	MEle = M, BcDis = N	MHV = H	0.6012	0.1103	16	34
	17	MEle = M, RDen = H, MsDis = N	MHV = H	0.5942	0.1033	17	37
	18	MEle = M, RDen = H	MHV = H	0.5917	0.1008	18	38
	19	MEle = M, BDen = H	MHV = H	0.5873	0.0964	19	39
	20	MEle = M, SmDis = N	MHV = H	0.5696	0.0787	20	42
	21	MEle = M, MsDis = N	MHV = H	0.5453	0.0544	21	45

Table 8. *Cont.*

Root Node	Number	Evidence (E)	MAP	P (MAP | E)	Degree of Influence	Group Ranking	Overall Ranking
	22	MEle = M	MHV = H	0.5350	0.0441	22	46
	23	MEle = M, BRDen = H	MHV = H	0.5331	0.0422	23	47
SLO	24	SLO = M, IDen = H, RDen = H, SmDis = N, BcDis = N	MHV = H	0.7236	0.2327	1	9
	25	SLO = M, IDen = H, RDen = H, MsDis = N, BcDis = N	MHV = H	0.7191	0.2282	2	10
	26	SLO = M, IDen = H, RDen = H, BcDis = N	MHV = H	0.6939	0.2030	3	13
	27	SLO = M, IDen = H, RDen = H, SmDis = N	MHV = H	0.6573	0.1664	4	22
	28	SLO = H, IDen = H, RDen = H, MsDis = N	MHV = H	0.6333	0.1424	5	28
	29	SLO = M, IDen = H, RDen = H	MHV = H	0.6184	0.1275	6	30
	30	SLO = M, BcDis = N	MHV = H	0.6002	0.1093	7	35
	31	SLO = M, IDen = H	MHV = H	0.6046	0.1137	8	33
FDen	32	FDen = M, FAR = M, IDen = H, RDen = H, SmDis = N, BcDis = N	MHV = H	0.8172	0.3263	1	1
	33	FDen = M, FAR = M, IDen = H, RDen = H, MsDis = N, BcDis = N	MHV = H	0.7892	0.2983	2	2
	34	FDen = M, FAR = M, IDen = H, RDen = H, BcDis = N	MHV = H	0.7757	0.2848	3	4
FDen	35	FDen = M, FAR = M, IDen = H, RDen = H, SmDis = N	MHV = H	0.7264	0.2355	4	8
	36	FDen = M, FAR = M, SCR = H, BcDis = N	MHV = H	0.6830	0.1921	5	15
	37	FDen = M, FAR = M, IDen = H, RDen = H	MHV = H	0.6733	0.1824	6	16
	38	FDen = M, FAR = M, IDen = H, RDen = H, MsDis = N	MHV = H	0.6708	0.1799	7	17
	39	FDen = M, FAR = M, FDiv = H	MHV = H	0.6646	0.1737	8	20
	40	FDen = M, FAR = M, IDen = H	MHV = H	0.6524	0.1615	9	23
	41	FDen = M, Bden = H, SCR = H, BcDis = N	MHV = H	0.6444	0.1535	10	24
	42	FDen = M, SCR = H, BcDis = N	MHV = H	0.6405	0.1496	11	26
	43	FDen = M, FAR = M, BDen = M	MHV = H	0.5958	0.1049	12	36
	44	FDen = M, FAR = M	MHV = H	0.5848	0.0939	13	40
	45	FDen = M, BDen = H	MHV = H	0.5698	0.0789	14	41
	46	FDen = M, FDiv = H	MHV = H	0.5646	0.0737	15	43
	47	FDen = M	MHV = H	0.5534	0.0625	16	44

Note: H stands for high, L stands for low, M stands for moderate, N stands for near, F stands for far and the degree of influence refers to the difference with the original probability of MHV = H.

In single-factor analysis, the probability of high street vitality was greatest when SLO was high. However, when SLO was combined with other factors, moderate SLO was required for greater probability of street vitality. In addition, there were many factor combination groups of SLO and MEle with the same nodes except the root node, such as factor combination groups 1 and 25. According to a comparison of these two groups, SLO played a relatively minor role in factor combination groups.

It is worth noting that in the single-factor analysis, the higher the building plot ratio, the greater the probability of high street vitality. However, when FAR was combined with FDen, moderate FAR stimulated the vitality of the street with a greater probability. The same situation existed with BDen. When BDen was combined with FAR and FDen, moderate BDen resulted in a combined factor group with a greater impact on street vitality. Therefore, in actual urban construction, BDen and FAR should not be as high as possible.

Excess building density could make people feel crowded and reduce the quality of the environment. Moderate BDen and FAR were more conducive to improving street vitality.

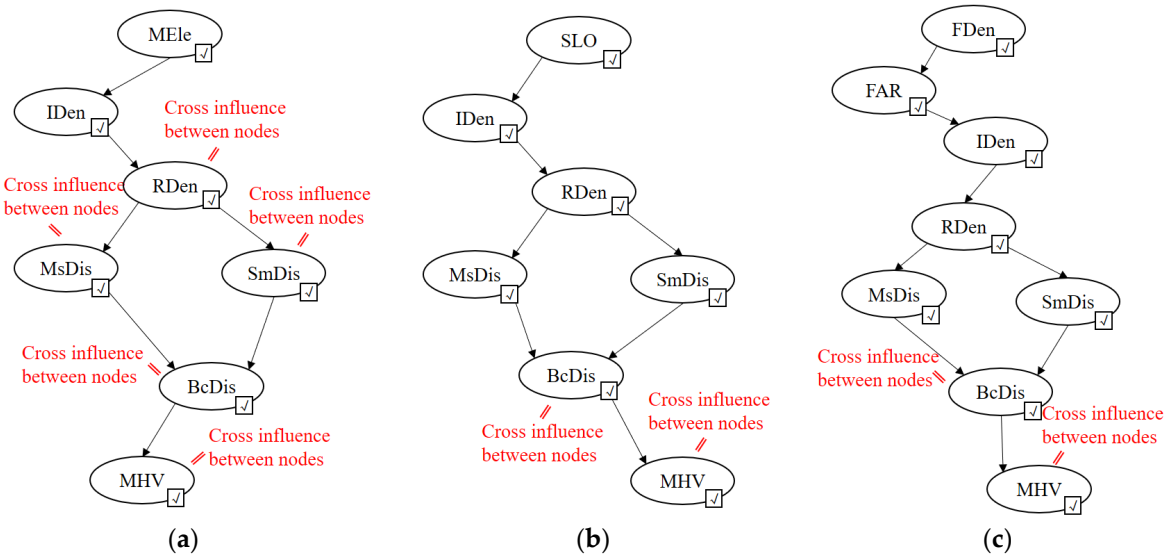

Figure 8. The longest path of the factor combination groups of different root nodes. (**a**) The longest path with MEle as the root node; (**b**) the longest path with SLO as the root node; (**c**) the longest path with FDen as the root node.

5. Discussion

5.1. Limitation and Further Possibilities of the Methodology Used in This Study

Firstly, the population activity data carried by Baidu LBS data were used as the external representation of street vitality in this study. Although these data are based on location data extracted from a large number of smartphone users, which can reflect the spatial distribution of population activity density in the same time period from a macro perspective, it is difficult to distinguish the crowd attributes and activity categories and to identify the trajectory of human activities. Secondly, based on relevant theories and previous studies, this study selected influencing factors from the aspects of horizontal interface characteristics, comfort, functionality, safety, location, accessibility, development intensity and street texture from two levels of street characteristics and street surrounding environment but more urban elements. Urban natural landscape, historical culture and other factors, such as hydrophilicity, were not included in this study. Furthermore, this research was only based on the data of Chongqing's inner ring streets, and some conclusions may be particular to this city. Finally, in the construction of the Bayesian network structure, in order to guarantee the objectivity of the data, this study mainly relied on a data-driven network model but still on the basis of the consensus in the field of network structure that a small amount of adjusting and optimizing is preferable. Although the final build of the Bayesian network model and its validation achieved excellent performance, there is still a certain amount of subjectivity.

Based on the above discussion, further research will be carried out considering the following four aspects. Firstly, data with more accurate and detailed spatial resolution can be used to distinguish the attribute characteristics of crowds, and OD data can be used to analyze the activity trajectory of specific crowds, their habits, preferences and other characteristics. The influence of seasonal factors on street vitality should also be considered. In addition, street view images and machine learning models can be used to obtain the ratings of streets based on people's subjective feelings to make up for the shortcomings of existing research. Secondly, in this paper, mainly selected influencing factors based on urban elements, but natural scenery, cultural characteristics and historical landscape in cities are also important factors for people's cognition of the urban environment, which

affects people's behavior. Subsequently, it is necessary to further explore the natural scenery, history and culture of cities to construct a more perfect influencing factor system of street vitality to make the research more scientific. Thirdly, this study took the Chongqing urban area as an example to carry out research, which may have resulted in conclusion particular to that city. In order to study the influence mechanism of street vitality in mountain cities with more universality, the research scope can be further expanded to select more mountain cities for research. In addition, with the continuous expansion of the research scope, the data scale will also continue to expand, and a Bayesian network model can be obtained only based on data learning to make the research results more objective. Finally, in this paper, living streets were studied, although they can be further subdivided according to their different functions and land use types, such as commercial streets, residential streets and mixed streets. Different types of streets may have different influencing factors and influencing mechanisms, so more detailed studies are needed in the future.

5.2. Possible Innovations in This Study

Based on a geographic information system, this study used Baidu heat map data, POI data, street map data, urban spatial data (road network data, building data, elevation data and bus routes) and multisource data to construct a street dynamic measurement of influencing factors based on the database for street vitality and the influence factors of quantitative analysis. A Bayesian network was introduced into the study to explore and analyze the relationship between the influencing factors and the influencing mechanism of street vitality based on the database.

This study conducted targeted research on mountain cities and preliminarily explored the causal relationship among the influencing factors. Taking the streets of mountain cities as the research object, an influencing factor system of street vitality suitable for mountain cities was constructed. Taking the data of Chongqing, a typical mountain city, as an example, a Bayesian network model was constructed. Based on the established model, we identified different types of influencing factors, preliminarily explored the correlation between the influencing factors and the influencing path and discriminated the influencing mechanism of street vitality in mountain cities in order to apply this model to other similar areas to help in decision making.

6. Conclusions

The key mechanisms of the influence of the physical environment of street space on street vitality are explained here. According to our analysis, the influence mechanism revolves around the function density and intersection density. On the one hand, it refers to the influence of the street and the built environment on either side of the street centered on functional density. On the other hand, it refers to the influence of other elements in the city centered on intersection density.

The influence mechanism from the perspective of self-environment mainly refers to the characteristics of the street itself and the built environment on both sides of the street in relation to street vitality, with FDen as the core, focusing on the street's function, safety and development intensity of both sides of the street. In urban construction, functional planning should be carried out on the basis on functional positioning. Functional density is related to the development intensity on both sides of the street. When the functional density of the street increases in order to support more functions of the street, there needs to be enough building space. Therefore, the size of buildings on both sides of the street will gradually increase, and the building density will also gradually increase. Excessive development intensity causes congestion and deteriorates the street environment, which in turn can inhibit street vitality. For efficient use of land while ensuring the comfort of the street, the building floor area ratio should also be kept at an appropriate level. The density of functions and sufficient building space promote the mixed use of functions, which can attract people with different needs to carry out activities on the street. After meeting basic functional needs, higher requirements will be put forward on the street environment.

A proper sense of enclosure of street space brings a sense of psychological security and comfort, which is mainly created by the forest of buildings and trees, thus attracting more people to carry out activities on the street and gradually forming street vitality.

The influence mechanism of the external environment perspective mainly refers to the influence of elements a certain distance from the street or within the larger buffer zone of the street on street vitality. This mechanism is based on the average elevation and functional density of the street, with the density of intersections around the street as the core and accessibility and location as the guarantee. Although the average elevation is a characteristic of the street itself, this factor has an impact on the construction around the street. During the construction of mountainous cities, more consideration should be given to geological and topographical factors. Areas with moderate elevations are generally located between rivers and mountains. Although there are some slope undulations, it is relatively easy to build and more convenient for people's life. Due to the influence of terrain in mountain cities, relatively few places are available for development and construction. In order to use the land as efficiently as possible, the construction granularity and the block divisions should be finer in places where the terrain is relatively flat and less difficult to develop, so the density of intersections and roads is greater. On the other hand, a rise in functional density leads to an increase in the building floor area ratio. In order to avoid overcrowding of functions and buildings while meeting the travel needs of more people, block division will is more detailed when buildings are gathered, resulting an increase in intersection density and road density. Small blocks and well-organized road networks result in less resistance for urban residents to come and more opportunities for social interaction activities. In response to the daily needs of people, shopping centers with a certain radiation range should be established in the area. Shopping centers and high road densities can attract residents who live far away from the city. The coverage of public transportation such as subways should be more scientific and reasonable, thus reducing the resistance of residents to travel for the same reason. On the basis of the increase in accessibility, the gradual increase in various functions carried by buildings and the gathering of shopping centers, there is a high probability of forming a commercial center that can play a radiating role in the surrounding streets, thus attracting more people to carry out activities in the streets and progressively stimulating the vitality of the street.

The above two modes of influence do not exist independently but should promote and complement each other in practice. It should be noted that the influence described in this study is a probabilistic causality. That is, the occurrence of A will lead to an increase in the probability of the occurrence of B, but the occurrence of A will not necessarily cause B to occur. In addition, for shorter time segments, the street spatial environment and the street vitality are mutually causal and continuous replacement. However, on the whole, it is the physical environment of the street that serves as the carrier. People then gather and carry out communication activities in the physical environment, thus forming the vitality of the street.

Author Contributions: Conceptualization, H.W. and P.X.; methodology, H.W. and J.T.; writing—original draft preparation, H.W.; writing—review and editing, R.C. and H.Y.; visualization, P.X.; supervision, P.X.; funding acquisition, P.X. All authors have read and agreed to the published version of the manuscript.

Funding: This research was funded by Chongqing University (grant number No. 2021CDJSKJC18) as part of the project, "Fundamental Research Funds for the Central Universities".

Institutional Review Board Statement: Not applicable.

Informed Consent Statement: Not applicable.

Conflicts of Interest: The authors declare no conflict of interest.

Appendix A. Calculation Method of Influencing Factors of Street Vitality

(1) Horizontal interface characteristics

a. SLen (Street length)

Where street length is the most basic physical property of a street. Street length can be directly calculated geometrically in Arcgis and expressed by SLen.

b. MEle (Elevation)

Street elevation measures the average elevation of a street, calculated by the following formula:

$$\mathrm{MEle} = \sum \mathrm{elevation_i}/\mathrm{n}\ (\mathrm{i} = 1, 2, \cdots, \mathrm{n})$$

where MEle is the average elevation of a certain street segment, $\mathrm{elevation_i}$ is the elevation of elevation point I in the buffer zone of about 10 m of the street segment and n is the total number of elevation points.

c. SLO (Slope)

$$\mathrm{SLO} = (\mathrm{Emax} - \mathrm{Emin})/\mathrm{length}$$

where SLO is the slope of a street segment, Emax is the maximum elevation value in the buffer zone of about 5 m of the street segment, Emin is the minimum elevation value in the buffer zone of about 5 m of the street segment and length is the length of the street segment.

(2) Comfortability

a. GVR (green view ratio)

In this paper, the proportion of green plants in street view images was used to measure the greenness; the calculation formula is as follows:

$$\mathrm{GVR} = \frac{\sum_i^n (\mathrm{fgvr_i} + \mathrm{hgvr_i})}{2\mathrm{n}}\ (\mathrm{i} = 1, 2, \cdots, \mathrm{n})$$

where $\mathrm{fgvr_i}$ is the proportion of green plants in the street view image in the direction of 0° of the I sample point, $\mathrm{hgvr_i}$ is the proportion of green plants in the street view image in the direction of 180° of the i sample point and n is the number of street view sample points on a given street segment.

b. SVR (sky view rate)

In this paper, the proportion of the visible sky area in the street view image to the overall picture was used to measure the openness of the street. The calculation formula is as follows:

$$\mathrm{SVR} = \frac{\sum_i^n (\mathrm{fk_i} + \mathrm{hk_i})}{2\mathrm{n}}\ (\mathrm{i} = 1, 2, \cdots, \mathrm{n})$$

where $\mathrm{fk_i}$ is the proportion of sky in the street view image in the direction of 0° of the ith sample point, $\mathrm{hk_i}$ is the proportion of sky in the street view image in the direction of 180° of the ith sample point and n is the number of sample points on a given street segment.

(3) Mixed use of function

a. FDen (functional density)

$$\mathrm{FDen} = \mathrm{n}/\mathrm{length}$$

where n is the number of POIs (points of interest) in the 50 m buffer of the street segment, and length is the length of the street segment.

b. FDiv (functional diversity)

$$\mathrm{FDiv} = \sum_i^n \mathrm{p_i} \times \ln \mathrm{p_i}\ (\mathrm{i} = 1, 2, \cdots, \mathrm{n})$$

where n is the number of POI categories in the 50 m buffer zone of a given street segment, and $\mathrm{p_i}$ is the ratio of a certain type of POI to the total number of POIs in the street segment. Public facility service POIs do not participate in the calculation of function mixing degree.

(4) Safety

a. SCR (surround close rate)

In this paper, the area proportion of vertical boundaries (buildings, walls and trees) in street images was used to measure the enclosure degree; the calculation formula is as follows:

$$SCR = \frac{\sum_i^n (fw_i + hw_i)}{2n} \ (i = 1, 2, \cdots, n)$$

where fw_i is the proportion of the vertical boundary in the street view image in the direction of 0° of the ith sample point, hw_i is the proportion of the vertical boundary in the street view image in the direction of 180° of the ith sample point and n is the number of street view sample points on this street segment.

b. LFac (lighting facilities)

In this paper, whether there is was street lamp in the street view was used to measure this index. It is expressed by LFac; 1 means existence, and 0 means non-existence.

(5) Location

a. BcDis (distance to nearest business center)

In this paper, Arcgis was used to directly calculate the straight-line distance between the center point of each street and the commercial center by using the "nearest neighbor analysis" tool, which is expressed by BcDis.

b. SmDis (distance to nearest shopping mall)

In this paper, the "nearest neighbor analysis" tool was directly used in Arcgis to calculate the straight-line distance between the center point of each street and the nearest shopping center, which is expressed by SmDis.

(6) Accessibility

a. BsDen (bus stop density)

Bus stop density refers to the ratio of the number of bus stops along a street segment to the street length and is used to measure accessibility by bus. The calculation formula is as follows:

$$BsDen = nlength$$

where n is the number of bus stops in the 55 m buffer zone around the street segment, and length is the length of the street segment.

b. BrDen (bus route density)

Bus route density refers to the ratio of the total bus route length covering the street to the length of the street and is also used to measure accessibility by bus. The calculation formula is as follows:

$$BrDen = length_b / length$$

where $length_b$ is the total length of all bus lines in the 55 m buffer zone around the block, and length is the length of the block.

c. MsDis (distance to nearest metro station)

In this paper, the "nearest neighbor analysis" tool was directly used in Arcgis to calculate the straight-line distance between the center point of each street and the nearest subway station, which is expressed by MsDis.

Road density refers to the ratio of the sum of road lengths within a certain area around the street to the area within this area; the calculation formula is as follows:

d. RDen (road density)

Road density refers to the ratio of the sum of road lengths within a certain area around the street to the area within this area, and the calculation formula is as follows:

$$RDen = l / area$$

where l is the length of the road in the buffer zone of about 1000 m, and area is the area of the buffer zone.

(7) Intensity of surrounding development

a. BDen (building density)

Building density refers to the ratio of the sum of the area under the building in the street buffer zone to the area of the street buffer zone; the calculation formula is as follows:

$$\mathrm{BDen} = \sum_{i}^{n} s_i / \mathrm{area}\ (i = 1, 2, \cdots, n)$$

where s_i is the floor area of a building in the 50 m buffer zone, n is the number of buildings in the buffer zone and area is the area of the buffer.

b. FAR (building floor area ratio)

Building floor area ratio refers to the ratio of the total building area in the street buffer zone to the street buffer area; the calculation formula is as follows:

$$\mathrm{FAR} = \sum_{i}^{n} s_i \times f_i / \mathrm{area}\ (i = 1, 2, \cdots, n)$$

where s_i refers to the floor area of the ith building in the 50 m buffer zone around the street segment, f_i refers to the number of the ith building floor, n is the number of buildings in the buffer and area is the area of the buffer.

(8) Street texture

IDen (intersection density) is the ratio of the number of intersections within a given perimeter of a street to its area, calculated as follows:

$$\mathrm{IDen} = n / \mathrm{area}$$

where n is the number of intersections in the buffer zone of 1000 m, and area is the buffer zone area.

Appendix B

Table A1. Discretization methods of Bayesian network node variables.

Node Variable	Value Range	Discrete Points	Discrete State
SLen	[20.0932, 716.7265]	213.5299, 405.4799	1 = short, 2 = moderate, 3 = long
Mele	[164.5557, 411.8496]	247.9944, 303.6890	1 = low, 2 = moderate, 3 = high
SLO	[0.0000, 0.6086]	0.0682, 0.1794	1 = low, 2 = moderate, 3 = high
GVR	[0.0016, 0.8578]	0.2352, 0.4494	1 = low, 2 = moderate, 3 = high
SVR	[0.0000, 0.6329]	0.2352, 0.4494	1 = low, 2 = moderate, 3 = high
FDen	[0.0000, 1953.2066]	206.2459, 602.9701	1 = low, 2 = moderate, 3 = high
FDiv	[0.0000, 2.3844]	0.7385, 1.5838	1 = low, 2 = moderate, 3 = high
SCR	[0.0692, 0.9246]	0.4361, 0.6107	1 = low, 2 = moderate, 3 = high
LFac	Discrete data	Discrete data	0 = none, 1 = exist
BcDis	[0.0000, 9624.5830]	1434.5387, 3235.9474	1 = near, 2 = moderate, 3 = far
SmDis	[16.9713, 6007.8322]	950.2655, 2041.5915	1 = near, 2 = moderate, 3 = far
BsDen	[0.0000, 0.0622]	0.0022, 0.0084	1 = low, 2 = moderate, 3 = high
BrDen	[0.0000, 39.5468]	2.2026, 6.8567	1 = low, 2 = moderate, 3 = high
MsDis	[1.4028, 2052.0572]	391.4430, 765.3989	1 = near, 2 = moderate, 3 = far
RDen	[1.0888, 9.1561]	4.9703, 6.5272	1 = low, 2 = moderate, 3 = high
BDen	[0.0000, 0.9706]	0.3299, 0.7698	1 = low, 2 = moderate, 3 = high
FAR	[0.0000, 31.9485]	3.9370, 11.8514	1 = low, 2 = moderate, 3 = high
IDen	[2.2676, 39.8717]	15.5843, 24.1685	1 = low, 2 = moderate, 3 = high
MHV	[51.0000, 192.0000]	165.1358	1 = low, 2 = high

References

1. Jacob, J. *The Death and Life of Great American Cities*; Modern Library: New York, NY, USA, 1993; p. 2.
2. Gehl, J.; Gemze, L. Public Spaces—Public Life. *Urban Des. Int.* **1996**, *2*, 1.
3. Montgomery, J. Making a city: Urbanity, vitality and urban design. *J. Urban. Des.* **2007**, *3*, 93–161. [CrossRef]

4. Jalaladdini, S.; Oktay, D. Urban Public Spaces and Vitality: A Socio-Spatial Analysis in the Streets of Cypriot Towns. In Proceedings of the Asia Pacific International Conference on Environment-Behaviour Studies (AicE-Bs), Famagusta, Cyprus, 7–9 December 2011. [CrossRef]
5. March, A.; Rijal, Y.; Wilkinson, S. Measuring Building Adaptability and Street Vitality. *Plan. Pract. Res.* **2012**, *27*, 1–22. [CrossRef]
6. Samvati, S.; Nikookhooy, M.; Saiedizadi, M. The Role of Vitality and Viability of Urban Streets in Enhancement the Quality of Pedestrian—Oriented Urban Venues (Case Study: Buali Sina Street, Hamedan, Iran). *J. Basic Appl. Sci. Res.* **2013**, *3*, 554–561.
7. De Nadai, M.; Staiano, J.; Larcher, R.; Sebe, N.; Quercia, D.; Lepri, B. The Death and Life of Great Italian Cities: A Mobile Phone Data Perspective. In Proceedings of the 25th International Conference on World Wide Web (WWW), Montreal, QC, Canada, 11–15 May 2016. [CrossRef]
8. Tu, W.; Zhu, T.; Xia, J.; Zhou, Y.; Lai, Y.; Jiang, J.; Li, Q. Portraying the spatial dynamics of urban vibrancy using multisource urban big data. *Comput. Environ. Urban Syst.* **2020**, *80*, 101428. [CrossRef]
9. Hasan, S.; Satish, V. Urban activity pattern classification using topic models from online geo-location data. *Transp. Res. Part C-Emerg. Technol.* **2014**, *44*, 363–381. [CrossRef]
10. Kim, K.-S.; Kojima, I.; Ogawa, H. Discovery of local topics by using latent spatio-temporal relationships in geo-social media. *Int. J. Geogr. Inf. Sci.* **2016**, *30*, 1899–1922. [CrossRef]
11. Liu, X.; He, J.; Yao, Y.; Zhang, J.; Liang, H.; Wang, H.; Hong, Y. Classifying urban land use by integrating remote sensing and social media data. *Int. J. Geogr. Inf. Sci.* **2017**, *31*, 1675–1696. [CrossRef]
12. Tussyadiah, I.P. A Concept of Location-Based Social Network Marketing. *J. Travel Tour. Mark.* **2012**, *29*, 205–220. [CrossRef]
13. Jin, X.; Long, Y.; Sun, W.; Lu, Y.; Yang, X.; Tang, J. Process funding Evaluating cities' vitality and identifying ghost cities in China with emerging geographical data. *Cities* **2017**, *63*, 98–109. [CrossRef]
14. Lin, L.; Moudon, A.V. Objective versus subjective measures of the built environment, which are most effective in capturing associations with walking? *Health Place* **2010**, *16*, 339–348. [CrossRef] [PubMed]
15. Ewing, R.; Handy, S.; Ross, C.B.; Clemente, O.; Winston, E. Identifying and Measuring Urban Design Qualities Related to Walkability. *J. Phys. Act. Health* **2006**, *3*, S223–S240. [CrossRef] [PubMed]
16. Yue, Y.; Zhuang, Y.; Yeh, A.G.O.; Xie, J.; Ma, C.; Li, Q. Measurements of POI-based mixed use and their relationships with neighbourhood vibrancy. *Int. J. Geogr. Inf. Sci.* **2017**, *31*, 658–675. [CrossRef]
17. Wu, C.; Ye, X.; Ren, F.; Du, Q. Check-in behaviour and spatio-temporal vibrancy: An exploratory analysis in Shenzhen, China. *Cities* **2018**, *77*, 104–116. [CrossRef]
18. Ye, Y.; Richards, D.; Lu, Y.; Song, X.; Zhuang, Y.; Zeng, W.; Zhong, T. Measuring daily accessed street greenery: A human-scale approach for informing better urban planning practices. *Landsc. Urban Plan.* **2019**, *191*, 103434. [CrossRef]
19. Chang, X.; Yeh, A.G.; Zhang, A. Analyzing spatial relationships between urban land use intensity and urban vitality at street block level: A case study of five Chinese megacities. *Landsc. Urban Plan.* **2020**, *193*, 103669. [CrossRef]
20. Mehta, V. Lively Street: Determining environmental characteristic to support social behavior. *J. Plan. Educ. Res.* **2007**, *27*, 165–187. [CrossRef]
21. Gehl, J.; Kaefer, L.J.; Reigstad, S. Close encounters with buildings. *Urban Des. Int.* **2006**, *11*, 29–47. [CrossRef]
22. Xu, X.; Xu, X.; Guan, P.; Ren, Y.; Wang, W.; Xu, N. The Cause and Evolution of Urban Street Vitality under the Time Dimension: Nine Cases of Streets in Nanjing City, China. *Sustainability* **2018**, *10*, 2797. [CrossRef]
23. Borst, H.C.; Miedema, H.M.E.; de Vries, S.I.; Graham, J.M.A.; van Dongen, J.E.F. Relationships between street characteristics and perceived attractiveness for walking reported by elderly people. *J. Environ. Psychol.* **2008**, *28*, 353–361. [CrossRef]
24. Harvey, C.W. Measuring Streetscape Design for Livability Using Spatial Data and Methods. Master's Thesis, State Agricultural College, University of Vermont, Ann Arbor, MI, USA, 16 July 2014.
25. Sarkar, C.; Webster, C.; Pryor, M.; Tang, D.; Melbourne, S.; Zhang, X.; Liu, J. Exploring associations between urban green, street design and walking: Results from the Greater London boroughs. *Landsc. Urban Plan.* **2015**, *143*, 112–125. [CrossRef]
26. Ye, Y.; van Nes, A. Quantitative tools in urban morphology: Combining space syntax, spacematrix and mixed-use index in a GIS framework. *Urban Morphol.* **2014**, *18*, 97–118.
27. Gil, E.; Ahn, Y.; Kwon, Y. Tourist Attraction and Points of Interest (POIs) Using Search Engine Data: Case of Seoul. *Sustainability* **2020**, *12*, 17. [CrossRef]
28. Li, X.; Zhang, C.; Li, W.; Ricard, R.; Meng, Q.; Zhang, W. Assessing street-level urban greenery using Google Street View and a modified green view index. *Urban For. Urban. Green.* **2015**, *14*, 675–685. [CrossRef]
29. Zhang, F.; Wu, L.; Zhu, D.; Liu, Y. Social sensing from street-level imagery: A case study in learning spatio-temporal urban mobility patterns. *ISPRS-J. Photogramm. Remote Sens.* **2019**, *153*, 48–58. [CrossRef]
30. Chen, L.; Lu, Y.; Sheng, Q.; Ye, Y.; Wang, R.; Liu, Y. Estimating pedestrian volume using Street View images: A large-scale validation test. *Comput. Environ. Urban Syst.* **2020**, *81*, 101481. [CrossRef]
31. Zeng, C.; Song, Y.; He, Q.; Shen, F. Spatially explicit assessment on urban vitality: Case studies in Chicago and Wuhan. *Sustain. Cities Soc.* **2018**, *40*, 296–306. [CrossRef]
32. Sahu, A.R.; Palei, S.K. Real-time fault diagnosis of HEMM using Bayesian Network: A case study on drag system of dragline. *Eng. Fail. Anal.* **2020**, *118*, 104917. [CrossRef]

33. Alobaidi, A.; Mahmood, N.T. Modified Full Bayesian Networks Classifiers for Medical Diagnosis. In Proceedings of the 2013 International Conference on Advanced Computer Science Applications and Technologies (ACSAT), Kuching, Malaysia, 23–24 December 2013.
34. Spyroglou, L.I.; Spock, G.; Rigas, A.G.; Paraskakis, E.N. Evaluation of Bayesian classifiers in asthma exacerbation prediction after medication discontinuation. *BMC Res. Notes* **2018**, *11*, 522. [CrossRef]
35. Dlamini, W.M. A Bayesian belief network analysis of factors influencing wildfire occurrence in Swaziland. *Environ. Model. Softw.* **2010**, *25*, 199–208. [CrossRef]
36. Furlan, E.; Slanzi, D.; Torresan, S.; Critto, A.; Marcomini, A. Multi-scenario analysis in the Adriatic Sea: A GIS-based Bayesian network to support maritime spatial planning. *Sci. Total Environ.* **2020**, *703*, 134972. [CrossRef] [PubMed]
37. Chee, Y.E.; Wilkinson, L.; Ann, E.N.; Pedro, F.Q.; John, E.F.; Hall, D.; Kimberli, J.P.; Rumpff, L. Modelling spatial and temporal changes with GIS and Spatial and Dynamic Bayesian Networks. *Environ. Model. Softw.* **2016**, *82*, 108–120. [CrossRef]
38. Jaafari, A.; Gholami, D.M.; Eric, K.Z. A Bayesian modeling of wildfire probability in the Zagros Mountains, Iran. *Ecol. Inform.* **2017**, *39*, 32–44. [CrossRef]
39. Stelzenmueller, V.; Lee, J.; Garnacho, E.; Rogers, S.I. Assessment of a Bayesian Belief Network-GIS framework as a practical tool to support marine planning. *Mar. Pollut. Bull.* **2010**, *60*, 1743–1754. [CrossRef]
40. Pearl, J. Probabilistic reasoning in intelligent systems: Networks of plausible inference. *Comput. Sci. Artif. Intell.* **1988**, *70*, 1022–1027.
41. Dormann, C.; Elith, J.; Bacher, S.; Buchmann, C.; Carl, G.; Carre, G.; Jaime, R.G.M.; Gruber, B.; Lafourcade, B.; Pedro, J.L.; et al. Collinearity: A review of methods to deal with it and a simulation study evaluating their performance. *Ecography* **2013**, *36*, 27–46. [CrossRef]
42. Hair, J.F.; Black, W.C.; Babin, B.J.; Anderson, R.E.; Tatham, R.L. *Multivariate Data Analysis*, 6th ed.; Pearson Prentice Hall: Upper Saddle River, NJ, USA, 2006.
43. Cooper, G.F.; Herskovits, E. A bayesian method for the induction of probabilistic networks from data. *Mach. Learn.* **1992**, *9*, 309–347. [CrossRef]
44. Spirtes, P.; Glymour, C. An Algorithm for Fast Recovery of Sparse Causal Graphs. *Soc. Sci. Comput. Rev.* **1991**, *9*, 62–72. [CrossRef]
45. Dempster, A.P. Maximum likelihood from incomplete data via the EM algorithm. *Comput. Stat. Data Anal.* **1977**, *39*, 1–38. [CrossRef]
46. Lauritzen, S.L. The EM algorithm for graphical association models with missing data. *Comput. Stat. Data Anal.* **1995**, *19*, 191–201. [CrossRef]
47. Rodriguez, J.D.; Perez, A.; Lozano, J.A. Sensitivity Analysis of k-Fold Cross Validation in Prediction Error Estimation. *IEEE Trans. Pattern Anal. Mach. Intell.* **2010**, *32*, 569–575. [CrossRef] [PubMed]
48. Goutte, C.; Gaussier, E. A Probabilistic Interpretation of Precision, Recall and F-Score, with Implications for Evaluation. In *Advances in Information Retrieval*; Springer: Berlin/Heidelberg, Germany, 2005.
49. Bradley, A.P. The use of the area under the roc curve in the evaluation of machine learning algorithms. *Pattern Recognit.* **1997**, *30*, 1145–1159. [CrossRef]
50. Wu, W.; Wang, J.; Li, C.; Wang, M. *The Geography of City Liveliness and Consumption: Evidence from Location-Based Big Data*; Lse Research Online Documents on Economics; London School of Economics and Political Science, LSE Library: London, UK, 2016.
51. Zhang, J.; Heng, C.K.; Malone-Lee, L.C.; Hii, D.J.C.; Janssen, P.; Leung, K.S.; Tan, B.K. Evaluating environmental implications of density: A comparative case study on the relationship between density, urban block typology and sky exposure. *Autom. Constr.* **2012**, *22*, 90–101. [CrossRef]
52. Harvey, C.; Aultman-Hall, L.; Hurley, S.E.; Troy, A. Effects of skeletal streetscape design on perceived safety. *Landsc. Urban. Plan.* **2015**, *142*, 18–28. [CrossRef]
53. Lauritzen, S.L.; Spiegelhalter, D.J. Local Computations with Probabilities on Graphical Structures and Their Application to Expert Systems. *J. R. Stat. Soc.* **1988**, *50*, 157–224. [CrossRef]